International Soil and Water Conservation Research 8 (2020) 383–392

Contents lists available at ScienceDirect

International Soil and Water Conservation Research

journal homepage: www.elsevier.com/locate/iswcr

Original Research Article

The use of remote sensing to detect the consequences of erosion in gypsiferous soils

Maria Jose Marques [a, *], Ana Alvarez [a], Pilar Carral [a], Blanca Sastre [b], Ramón Bienes [b]

[a] Geology and Geochemistry Department, Autonomous University of Madrid, Calle Francisco Tomás y Valiente, 7, 28040, Madrid, Spain
[b] Department of Applied Research and Agrarian Extension, IMIDRA, Finca El Encín. Carretera A-2, Km 38.8. Alcalá de Henares, 28800, Madrid, Spain

ARTICLE INFO

Article history:
Received 13 February 2020
Received in revised form
25 September 2020
Accepted 8 October 2020
Available online 16 October 2020

Keywords:
Tillage
Erosion
NDVI
Gypsum
Remote sensing
Soil color

ABSTRACT

Tillage practices on sloping ground often result in unsustainable soil losses impairing soil functions such as crop productivity, water and nutrients storage, and soil organic carbon (SOC) sequestration. A sloping olive grove (10%) was planted in shallow gypsiferous soils in 2004. It was managed by minimum tillage; the most frequent management practice in central Spain. The consequences of erosion were studied in soil samples (at 0–10, 10–20, and 20–30 cm depths) by analyzing SOC, available water and gypsum content, and by detecting spectral signatures using an ASD FieldSpecPro® VIS/NIR-spectroradiometer. The Brightness index (BI), Shape index (FI), and Normalized Difference Vegetation Index (NDVI) were derived from the ASD spectral signatures and from remote sensing (Sentinel-2 image) data. The development of these young olive trees was estimated from the measured diameter of the trunks (17 ± 18 cm diameter). In 20–30 cm of the soil, the carbon stock (38 ± 18 Mg ha^{-1}) as well as the available water content (12 ± 6%) was scarce, affecting the productivity of the olive grove. The above-mentioned indices obtained from the laboratory samples and the pixels of the Sentinel-2 image were significantly ($p < 0.01$) correlated, with a correlation coefficient of around 0.4. The BI was related to the gypsum content and the slope of the plot. The FI was related to the carbon and water contents. The NDVI derived from the satellite image identified the influence of soil degradation on the trees and the carbon content. The spatial-temporal changes of the indices might help in tracking soil changes over time.

1. Introduction

Soil degradation is considered one of the most important environmental topics in recent years (Rojas et al., 2016) and has been studied under very different approaches and methodologies (Borrelli et al., 2017). Without a doubt, remote sensing is one of the most important tools to monitor soil changes, being increasingly used as image resolution has been improved. Since the initial research on the relationships between soil properties and spectral reflectance (Condit, 1970), many different studies have gathered different physical-chemical characteristics to build spectral libraries (Ben-Dor et al., 2008; Dematte et al., 2004; Shepherd & Walsh, 2002), in order to establish links between spectral signatures and different soil parameters such as texture (Castaldi et al., 2016), moisture (Whiting et al., 2004) or contents of different elements or compounds, like mineral composition (Sabins, 1999), salt concentration (Metternicht & Zinck, 2003), or organic carbon (Gomez et al., 2008). The VIS, NIR, and SWIR hyperspectral airborne data has been even used for the study of age and soil formation (Ben-Dor et al., 2006; Galvão et al., 2008). An important aspect of remote sensing or earth observation is its usefulness for land monitoring and environmental assessment (Dubovyk, 2017), as this information can be used to assist in the decision-making process to achieve global environmental protection and sustainable development.

This paper is addressing one of the problems of degradation of agricultural soils, erosion, and its repercussions on crop productivity, whose consequences are of particular importance (Panagos et al., 2015). The research involving earth observation systems and soil erosion is based on aerial photos and remote sensing satellite imagery. Different assessments are grounded on changes in vegetation cover (Dwivedi & Ramana, 2003; Symeonakis & Drake,

* Corresponding author.
E-mail addresses: mariajose.marques@uam.es (M.J. Marques), anamaria.alvarez@uam.es (A. Alvarez), pilar.carral@uam.es (P. Carral), blanca.esther.sastre@madrid.org (B. Sastre), ramon.bienes@madrid.org (R. Bienes).

https://doi.org/10.1016/j.iswcr.2020.10.001

List of abbreviations

ASD	analytical spectral device (ASD) spectroradiometer
AWC	available water capacity
BI	brightness index
FC	field capacity
FI	shape index
NDVI	normalized difference vegetation index
NIR	near infra-red
PWP	permanent wilting point
S-2	Sentinel 2
SOC	soil organic carbon
Sqr Gyp:	square root of gypsum content
VIS	visible

2004); changes in topography (Lee & Liu, 2001) and mass changes related to gully processes (Bennett & Wells, 2019; Bocco & Valenzuela, 1993). The different characteristics between eroded and depositional areas (Beaulieu & Gaonac'h, 2002) can be also used as indicators of erosion processes, for example, the relative abundance of different soil particle size, considered as a proxy of soil loss, has produced highly accurate results at the local scale (Hill et al., 1995). A wide review of factors involving erosion and remote sensing, mapping techniques and validation methods can be found in Vrieling (2006).

When soils are shallow and show well-defined horizons with different colors, erosion is clearly indicated by color changes in the ground surface. Color information can be retrieved from the VIS region of the electromagnetic spectrum, and in agricultural soils, it is usually related to soil organic carbon (SOC), textural properties (Castaldi et al., 2016; McCarty et al., 2002) and presence of salts, e.g. outcrops of subsurface horizons enriched with carbonates or gypsum (Escadafal, 1994). Color changes indicate a dual process; superficial horizons are lost at the same time that the layers underneath, with contrasting characteristics, are gradually emerging. As already mentioned, different physical-chemical characteristics can be detected by changes in reflectance and spectral signatures of soils. Remote observation of soils does not allow to calculate erosion rates, but it does allow to estimate different states of degradation of soils when color changes indicate that C horizons of soils approach the surface. This process usually entails changes in SOC, soil bulk density or nutrients that harm soil functions, especially primary productivity, edaphic biodiversity, and hydraulic properties. This causes problems in agricultural production and can lead to gradual land abandonment. Eventually, when these soils are definitely abandoned, spontaneous vegetation will also find difficulties to grow and land experiences a shift to irreversible degradation (D'Odorico et al., 2013).

In this study, differences in soil reflectance observed from satellite imagery were used to estimate soil degradation and loss of productivity in a sloping area used for olive production under semi-arid environmental conditions. Traditional olive orchards have been installed in sloping and poor gypsiferous soils and consequently have experienced high rates of soil erosion (Fleskens & Stroosnijder, 2007) being in conflict with environmental sustainability and hampering its conservation as a traditional agricultural system (de Graaff et al., 2008). More sustainable land use practices have been proposed (Gómez et al., 2003; Hernandez et al., 2005; Sastre et al., 2017), but farmers are reluctant to change their management practices (Marques et al., 2015). There is an urgent need to involve farmers in this effort to protect soil and maintain sustainable production. In order to do so, the consequences of soil erosion on agronomic productivity can be more effective than figures focused on soil erosion rates.

This paper was motivated by the need to highlight the influence of erosion on elements that are important for land users like agricultural productivity, water availability, and the ability to adapt to climate change in semi-arid areas. Soil loss studies in the region of central Spain (Marques et al., 2007; Bienes et al., 2009; Sastre, 2017) observed that erosion resulted in the exposure of the deeper soil horizon and arguably, the differences in soil properties could be detected by remote sensing. Based on plot-scale measurements, the present study intended to demonstrate the relationships between soil reflectance and i) soil characteristics: i.e., soil organic carbon content, water availability, and gypsum content, ii) plot slope, and iii) olive tree development.

2. Material and methods

2.1. Study area

The study area is located in a semi-arid Mediterranean environment in the Center of the Iberian Peninsula. In the last 20 years, the accumulated mean annual rainfall yields 380 mm (Source Meteorological Climate Agency). The area shows a rolling landscape where agricultural use is predominant, especially for growing olive groves and vineyards, and for grazing cattle. The tops of hills are colonized by species of scrubland well adapted to drought and gypsic soils such as the Poacea *Stipa tenacissima* (Fig. 1a).

The agricultural plot under study (Datum ETRS89, latitude: 40°4′25″N; longitude: 3°31′20″W) has gypsiferous soils. According to the FAO soil classification (WRB, 2015), two main soils can be distinguished: Haplic Gypsisols usually found in flat areas, and Gypsiric Regosols being shallow and located in sloping areas. Fig. 1 (b) shows these regosols with Cy1 horizon found by 35–40 cm depth having high gypsum contents. These horizons are very unfavorable for vegetation establishment. In previous research, soil study analyses demonstrated high susceptibility to erosion due to its silty loam texture (Sastre et al., 2017). This plot was previously used to grow vines, but in 2004, vines were unearthed and olive trees were planted (7 × 7m). The plot has been monitored since this implementation and several episodes of intense erosion have been recorded (Fig. 1 a). The plot covers 3.7 ha, with 10–12% of slope. The altitude above sea level ranges between 540 and 560 m. Soil is tilled two or three times a year using chisel plow up to 20 cm depth.

2.2. Soil sampling and soil variables

In the plot under study, 30 georeferenced samples were selected according to a randomized systematic design (Fig. 1 a, c). Around these soil samples, trees vigor was estimated by trunk diameter. The diameter of olive trees was estimated at each sampling point by averaging the tree's diameters of the four olive trees immediately around each point; the height of measurement was 1 ± 0.1 m, variations were due to branches impeding measurements. The olive trees were planted in 2004. Dead or defective trees were replaced in the next two years, therefore, at the time of sampling olive trees were between 12 and 15 years old.

Soil samples were taken in late summer of 2017, at three different depths (0–10; 10 to 20 and 20–30 cm). Soil samples were air-dried and sieved (2 mm). Two groups of subsamples were established, one group to measure physical-chemical variables and another one to obtain the spectral signatures using an analytical spectral device (ASD) spectroradiometer described below.

The first group of subsamples was used to measure available water capacity (AWC) using the pressure plate method (Richards,

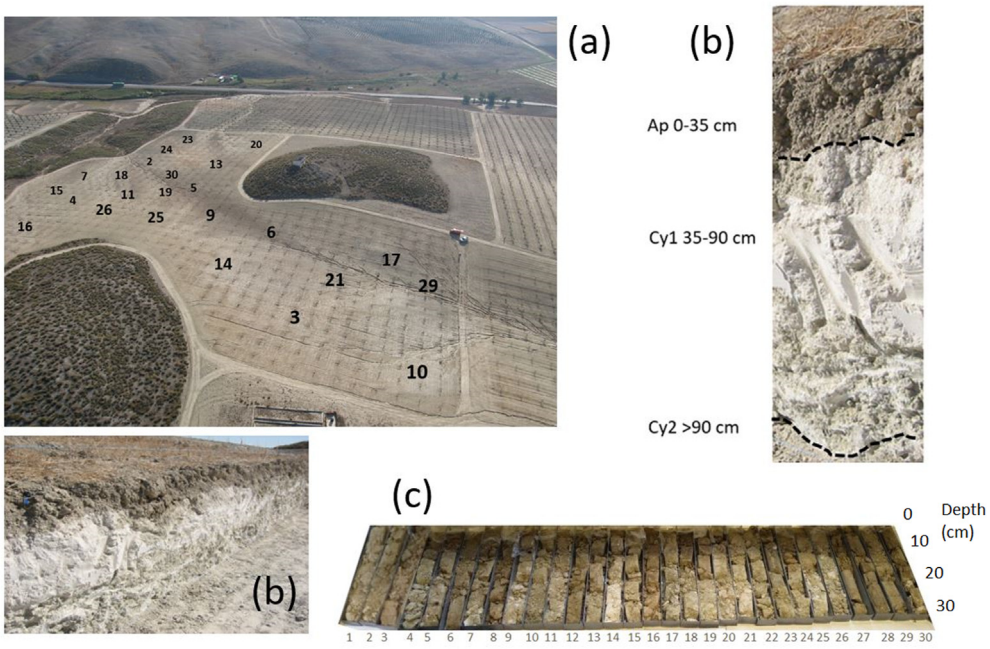

Fig. 1. Airborne photography of the study plot with sampling points a few days after a high-intensity rain event, the top of the hills are covered by spontaneous vegetation dominated by *Stipa tenacissima* species; throughout the cultivated slopes, rill erosion is clearly visible in different small watersheds on the plot (a). Representative soil profile (b), and thirty core samples from 0 to 30 cm depth (c).

1941), and gypsum content was estimated using X-ray diffraction analysis (Klug & Alexander, 1974). These subsamples were also used to measure soil organic carbon stock (Equation (1)).

$$\text{Soil.Organic.C.Stock.}\left(\text{Mg.ha}^{-1}\right). = \text{.SOC.(\%).} \times \text{.Bulk.density.}\left(\text{Mg m}^{-3}\right). \times \text{.depth.(m).x.100} \quad (1)$$

The SOC (%) was estimated by the Loss On Ignition Method (Schulte & Hopkins, 1996); soil bulk density was estimated as the mean density of 5 macroaggregates (1–3 cm diameter) obtained by the mercury-displacement method (Franklin, 1977). This method was accurate to measure the bulk density of irregular rocks using nominal diameters ranging from 2 to 3 cm (Franzini & Lezzerini, 2003). Large macroaggregates (0.8–1.9 cm) have been found to store and protect labile SOC and are good indicators of potential C responses to land use management changes (Tivet et al., 2013). The depth considered was 30 cm, following recommendations of the Intergovernmental Panel on Climate Change (IPCC, 2006). There were no gravel or stones in the study area.

The sieved dry samples of the second subset were placed on 5 cm diameter by 1 cm depth soil dishes to measure soil spectral signatures across 350–1100 nm using an ASD FieldSpecPro® VIS/NIR spectroradiometer (Boulder, CO, USA). The procedure was carried out in a dark room using the ASD contact probe (halogen bulb 2900K color temperature). Each scan was the 10 internal scan average. Noisy portions from 350 to 450 nm and 950–1100 nm were removed prior to statistical analysis. A white Spectralon™ was used every 9 measurements to optimize the spectroradiometer measurements. Hereinafter the indices, explained in section 2.4, calculated with laboratory ASD measurements will be qualified as "ASD".

Soil reflectance was obtained by two methods: laboratory spectroscopic measurements of soil samples (ASD) and spectra derived from the Sentinel 2 (S-2) multispectral image.

2.3. Images

One cloud-free Sentinel-2 image (Level 2) was downloaded from ESA Sentinels Scientific Data Hub, this image was obtained on the November 15, 2017, it was selected as the closest date from ground sampling without rain events in the previous three weeks. Fig. 3 depicts a detailed airborne image (pixel size 50 cm; planimetric precision 1m rmse), it was downloaded from the National aerial Orthophotography (Instituto Geográfico Nacional, 2014), the flight was made in the 2017 campaign. Images were analyzed with Open Source Geospatial Information System (QGIS., n.d.) and the Sentinel Application Platform v7.0 (SNAP-ESA. *Sentinel Application Platform v7.0.2*, n.d.).The remote sensing indices, explained in

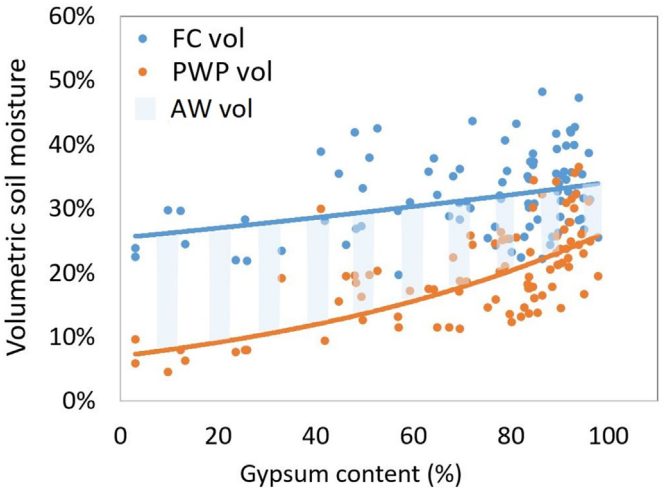

Fig. 2. Volumetric soil moisture at field capacity (FC vol) and Permanent Wilting point (PWP vol). The difference between these two measures results in the available water (AW vol). Changes according to the gypsum content in 90 soil samples.

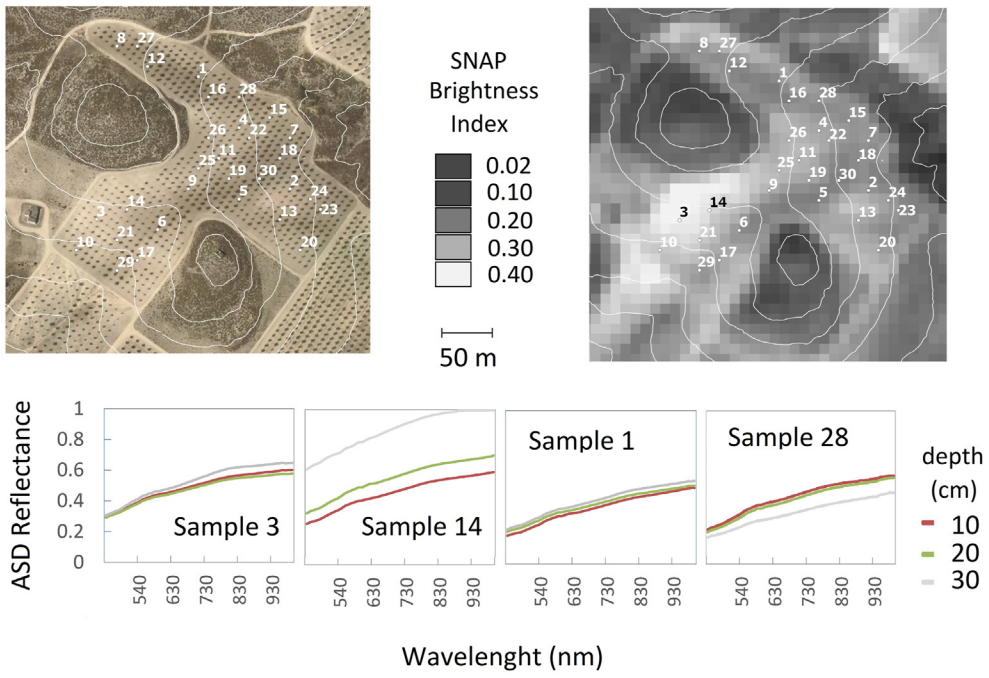

Fig. 3. Location of sampling points at the study plot. On the left aerial orthogonal image obtained in 2017 (latest images PNOA https://pnoa.ign.es/). On the right Sentinel-2 image Level 2. Brightness Index ("SNAP BI", Soil Radiometric Index. SNAP software). Below, four examples (samples No. 3, 14, 1 and 28) of spectral reflectance curves performed with the ASD spectroradiometer of samples taken at three different soil depth; 0 to 10 (red), 10 to 20 (green) and 20–30 cm (blue). The Y-axis shows Reflectance, the X-axis shows wavelength (nm).

section 2.4, were derived by ESA's SNAP Sentinel-2 Toolbox software. Hereinafter these indices will be qualified as "S-2".

2.4. The thematic indices

The visible and near infra-red (NIR) part of the electromagnetic spectrum was used to compute three different thematic indices. The Brightness Index (BI; Equation (2)) is related to the brightness of soils, which in turn is influenced by soil moisture, presence of salts and organic matter content of soil surface (Escadafal, 1989). The Shape index (IF; Equation (3)) is similar to a coloration index, it was proposed by Escadafal (1994) for the identification of degraded calcareous and gypsiferous soils in Tunisia. The normalized difference vegetation index (NDVI; Equation (4)) indicates the photosynthetic capacity or the energy absorbed by plant canopies, hence, the amount of healthy vegetation. This index can distinguish between soil and vegetation, minimizing topographic effect; however, the influence of soil background is significant (Huete et al., 1994). In arid and semi-arid environments with scarce vegetation, the NDVI index shows spectral properties of soils, and considering the visible range, it can be a proxy of environmental degradation (Escadafal et al., 1994, pp. 253–259); it varies between −1.0 and + 1.0.

$$BI = \sqrt{\left(R^2 + G^2\right)/2} \tag{2}$$

$$\mathrm{FI} \cdot \ = \cdot(2\mathrm{R} - \mathrm{G} - \mathrm{B})/(\mathrm{G} - \mathrm{B}), \tag{3}$$

$$\mathrm{NDVI} \cdot \ = \cdot(\mathrm{NIR} - \mathrm{R})/(\mathrm{NIR} + \mathrm{R}) \tag{4}$$

where the letters refer to the reflectance values acquired in the blue (B, Band 2, 490 nm); green (G, Band 3; 560 nm); red (R, Band 4; 665 nm); and near-infrared (NIR, Band 8; 842 nm) wavebands (ESA, 2015).

2.5. Statistical analyses

The Gaussian distribution of soil variables was checked; only the gypsum content was transformed using the square root of the variable to approximate to a Normal distribution. Parametric analyses were used to calculate descriptive statistics and correlations between variables. Significant differences between soil layers were estimated by one way ANOVA and Kolmogorov-Smirnov test for parametric and non-parametric distributions respectively. A principal component analysis (PCA) was used to reduce the dimensions of data sets and find out Components or Factors with the highest variance. The SPSS software was used to perform statistical analysis (SPSS-Inc., 2009).

3. Results

3.1. Soil organic carbon, water, and gypsum

Table 1 shows significant differences across the three soil layers studied. The first two layers: 0 to 10 and 10–20 cm are similar, but they are different from the deeper layer (20–30 cm), which shows less carbon, higher bulk density, and less available water content. Gypsum content was also significantly higher at the deepest layer. Gypsum values have been expressed with the median and quartiles and the significant differences established by non-parametric tests.

Soil bulk density and gypsum concentration are increasing simultaneously with depth. Any increase in these variables, which may be found in deeper soil layers (Tables 1, 20–30 cm depth), have significant effects on water content; however, only gypsum content shows significant negative correlation with plant available water in this soil. The relationship between these two variables and water volume in soil can be observed in Table 2.

The influence of gypsum on water availability can be seen in Fig. 2. In these soils, higher gypsum content fundamentally affects

Table 1
Mean and standard deviation of soil parameters. FC = volumetric soil moisture at Field Capacity; PWP = volumetric soil moisture at Permanent Wilting Point. Gypsum concentration is described with the median and quartiles (Q25 and Q75) due to the lack of Normal distribution of this variable. Different letters indicate significant differences, $p < 0.05$.

Soil parameters at different depth	0–10 cm (n = 30)	10–20 cm (n = 30)	20–30 cm (n = 30)	Average 0–30 cm (n = 90)
SOC (g kg^{-1})	12.8 ± 4.2 a	10.9 ± 4.6 a	7.4 ± 4.8 b	10.4 ± 5.1
Bulk density (Mg m^{-3})	1.1 ± 0.2 a	1.2 ± 0.1 a	1.4 ± 0.2 b	1.2 ± 0.2
C Stock (Mg ha^{-1})	14.5 ± 5.3 a	12.6 ± 6.1 a	9.7 ± 6.4 b	37.8 ± 18.3
Water content at FC (%)	32 ± 5 a	30 ± 6 a	34 ± 7 a	32 ± 6
Water content at PWP (%)	17 ± 5 a	18 ± 6 a	24 ± 8 b	20 ± 7
Available Water (%)	14 ± 4 a	12 ± 5 a	10 ± 6 b	12 ± 6
Gypsum median (%)	80.7 (70–86) a	81.6 (61–89) a	89.3 (46–94) b	82 (59–90)

the volume of water available at the Permanent Wilting Point (PWP). As a result, the difference between Field Capacity (−33 kPa) and PWP (−1500 kPa) is getting smaller, and therefore the AWC is significantly affected. Arguably, the increase of gypsum content in topsoils, as a consequence of erosion processes, will influence water availability.

3.2. Soil reflectance and indices

It was hypothesized that erosion processes lead to the exposure of the deeper soil horizons, having low SOC and high gypsum content, and this different composition can be detected by soil reflectance. In these sloping plots, ASD measured reflectance allows soils to be classified into four general types, concerning their spectral signature. A group of soils having high reflectance, indicating low SOC content and high gypsum content, had spectral signatures like those located at the bottom left side of Fig. 3; among them, several soils had very similar reflectance for the three layers studied, such as the sample 3; other soils had the deepest layer (20–30 cm) very close to the Cy horizon, so that with high gypsum content, and very light colors, as was the case of sample 14 with high reflectance for the 20–30 cm layer. Another group of soils showed lower surface reflectance, indicating higher SOC and low gypsum content, in Fig. 3 they are located at the bottom right side, and once again, there were soils with the upper 30 cm very homogeneous, like sample 1; and other soils had less reflectance at the 20–30 cm layer, this would be the case of soils with a higher carbon content throughout the whole depth studied (from 0 to 30 cm).

Following the equations mentioned above, BI, FI and NDVI indices were calculated for ASD and S-2 reflectance. The figures obtained for these indices were different. Considering the significant differences between the two upper layers (0–10 and 10–20 cm) representing tilled soils, and the deeper one (from 20 to 30 cm depth) untilled, a correlation analysis between the variables considered in this study was divided into two blocks, surface soil, (0–20 cm) and the whole profile (0–30 cm). Table 3 shows the correlations between indices obtained by ASD measurements and the corresponding indices obtained from the reflectance of pixels in the S-2 image.

The pairs of indices obtained from S-2 and ASD are positively and significantly correlated, especially the FI_S-2 and FI-ASD, whose correlation is 0.49 for tilled layers. It is also noteworthy that for the indices calculated in soil samples from 0 to 30 cm depth the significance of correlation persisted, although diminished for NDVI and FI, but not so for BI.

Table 2
Correlations between bulk density and gypsum concentration (squared root) and water content of soils (FC: volumetric water content at Field Capacity; PWP: volumetric water content at Permanent Wilting Point).

Soil Parameters	Bulk density (n = 90)	Sqr Gypsum (n = 90)
Water content at FC (%)	R = 0.59; p < 0.001	R = 0.34; p = 0.001
Water content at PWP (%)	R = 0.47; p < 0.001	R = 0.64; p < 0.001
Plant Available Water (%)	R = 0.07; p = 0.52	R = − 0.44; p < 0.001

3.3. Relationships between soil reflectance and soil properties

Again, considering the significant differences between the two first layers and the at 20–30 cm depth, two principal component analysis (PCA) were performed separately, one of them with values obtained from 60 samples taken at 0 to 10 and 10–20 cm depth, and the other PCA analysis conducted with 30 samples taken from 20 to 30 cm depth. The slope at the sampling point position, the SOC estimated as C Stock, the volumetric AW and the gypsum content, transformed by square root (Sqr Gyp) were used as ground indicators. The olive tree trunk diameter, ranging from 7.6 to 22.5 cm, was a biological indicator of the influence of soil conditions. In this study, trunk diameter showed a positive correlation with C stock in soils (0–30 cm) ($r = 0.57$, $p < 0.01$), and negative with gypsum content ($r = -0.53$, $p < 0.01$). Finally the set of indirect indicators of soil condition: BI, FI, and NDVI, derived by S-2, and calculated from ASD measurements was also included. The objective was to determine the information that can be retrieved from these indices and the relationship between these indices obtained from different sources. Considering the topsoil or soil that was influenced by tillage (0–20 cm depth), Fig. 4 shows the projection of variables on the plane set by Factors 1 and 3 which extract 70% of the variance; it depicts the relationships between soil and vegetation variables and the group of Indices. Both brightness indices are on the right side of the factor plane, close to gypsum concentration and slope, with which they are related. On the opposite side, the magnitude of tree diameter, diametrically opposite to the Slope of the plot, is located close to the NDVI index obtained in the S-2 image. On the same side of the factor plane, we can find the C stock, close to both Shape indices (FI) and close to them the AWC, which is in turn, opposite to the gypsum content.

The contributions of variables on the PCA Factor coordinates based on correlations are shown in Table 4. The first PCA Factor is involving C stock, AWC, Olive trunk diameter, and NDVI and Shape indices, all of them are inversely related to gypsum content. According to this Factor, higher terrain slope tends to coincide with soils having higher gypsum content, less C stock and less water availability. These results are valid for both PCA analysis, 0 to 20 and 20–30 cm depth. In both cases, Factor 1 extracts 55% of the variance (Table 4). The indices obtained from ASD showed stronger correlations with this Factor than those obtained from S-2 images.

The second Factor of PCA is specifically related to the slope of the plot, with a weak relationship with the tree diameter, especially for the set of 20–30 cm depth. The third Factor is of special interest because it is made up by the simultaneous variations of tree diameter and water availability, being the other factors negligible,

Table 3
Correlations between indices. The remote sensing indices were calculated in the Sentinel-2 image (date 2017-11-15) with SNAP software. Brightness Index (BI_S-2), Shape Index (FI_S-2); Normalized Difference Vegetation Index (NDVI_S-2). The same indices were calculated from the blue, green, red and NIR wavelengths obtained with the analytical spectral device, BI_ASD; FI_ASD and NDVI_ASD. (*) Marked correlations are significant.

Indices	Depth 0–20 cm (tilled layers) N = 60			Depth 0–30 cm (both tilled and untilled) N = 90		
	NDVI_S-2	BI_S-2	FI_S-2	NDVI_S-2	BI_S-2	FI_S-2
NDVI_ASD	0.44 * $p < 0.001$			0.31 * $p < 0.005$		
BI_ASD		0.38 * $p < 0.005$			0.37 * $p < 0.005$	
FI_ASD			0.49 * $p < 0.001$			0.37 * $p < 0.001$

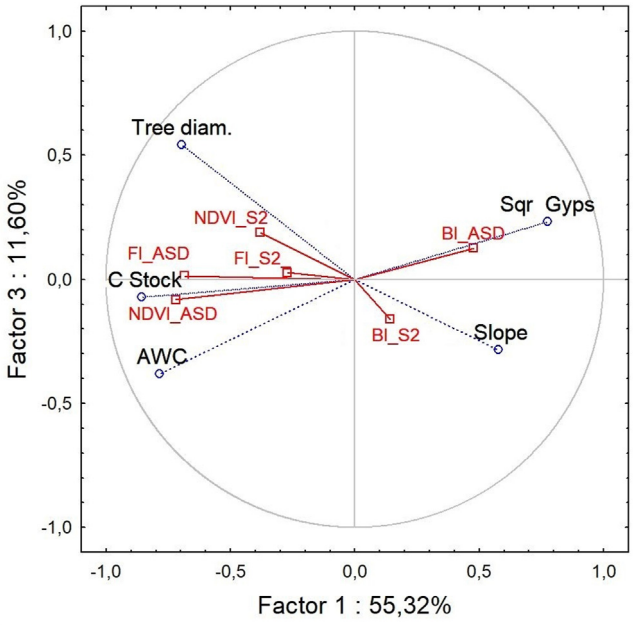

Fig. 4. Projection of variables on the plane formed with Factors 1 and 3. Physical-Chemical soil variables (tilled soil 0–20 cm depth) were carbon stock in Mg ha^{-1} (C-Stock); Available water capacity (AWC), Gypsum (Sqr Gyps). The slope and Tree Diameters were also considered. The indices calculated in the Sentinel-2 image (date 2017-11-15) with SNAP software were: Brightness Index (BI_S-2), Shape Index (FI_S-2); Normalized Difference Vegetation Index (NDVI_S-2). The same indices were calculated from the blue, green, red and infra-red wavelengths obtained with the analytical spectral device, BI_ASD; FI_ASD and NDVI_ASD. Factor 1 is related to slope and gypsum content. Factor 3 is related to olive tree diameter and water scarcity.

especially at the deepest layer. The information carried out by this third Factor is of concern in this water-scarce environment, so that Fig. 4 shows the spatial distribution of sampling points according to Factors 1 and 3 of the PCA. The figures show the two shallow layers separately from the deepest layer. First, we can observe the similar location of samples in the plane formed by these factors when layers are alike since the points usually appear very close. In red, the soils corresponded to 0–10 cm depth, and in green, soils were from 10 to 20 cm depth; this was expected given that there were no significant differences between them (Table 1). Factor 1, which extracts the maximum variance, is indicating the carbon content, the water content that is maximum to the left of the created space and is minimal on the right. Similarly, on this axis of Factor 1, on the left are the samples with the lowest gypsum content, and on the right, those with the highest gypsum content, which coincided with areas with greater slope. Factor 3, on the Y-axis, represents the health of the trees, which is measured indirectly through the diameter of the trunks, which is also related to the plant available water. This distribution of the PCA indicates that the most degraded soils are in the lower right quadrant.

When comparing charts in Fig. 5, we can observe that several soils appeared at approximately the same location in both analyses (charts a and b), this means that for these soil samples, the three layers were similar, for example, samples 4 or 17, always in the lower right quadrant, or samples 8 and 27 always in the lower left quadrant. When samples were placed in a different quadrant, there were more differences between the variables in surface and depth, as was the case of sample 14, whose spectral signature is also observed in Fig. 1, which shows more reflectance in the deepest layer, and therefore with greater gypsum content and less SOC.

It can also be noted that soil samples of the upper layers (0–10 and 10–20 cm depth) on the upper chart of Fig. 5 (a), are mainly located at the confluence of the axes, that is, this is a sample population of similar data, while in the deeper layer (20–30 cm) on the bottom chart of Fig. 5 (b), soil samples tend to appear scattered, and there are none in the central zone.

According to the PCA analysis, there is a link between soil brightness and gypsum content, similarly the FI index is related to the C stock and NDVI appears close to the variable of diameter of olive trees. Fig. 6 depicts soil and the tree variables studied in the first 20 cm, grouped according to regular intervals of the indices obtained from the pixels of the S-2 image, with which they can best be monitored. From left to right some soils have progressively more gypsum content (Fig. 6 a), less SOC (b) and a smaller diameter of the olive trees (c). Brightness values greater than 0.3 are an indicator of soil problems, which are reflected in a lower development of trees. The FI index, represented versus the C stock values, shows significant differences in SOC content from values of 2.4. The NDVI is the index that best represents the diameter of the olive trees, although significant differences appear only for values greater than 0.18.

4. Discussion

Erosion in the study area has been studied in recent years. The estimated soil loss was reported as 30 Mg ha^{-1} yr^{-1} (Sastre, 2017); moreover, losses of 93 Mg ha^{-1} were recorded after a single high-intensity precipitation event of 55 mm h^{-1} for 10 min (Bienes & Marques, 2008) leading to an average soil loss of 0.6 cm. Alarming amounts of annual erosion rates were noticed for other sloping olive groves managed by conventional tillage practices, for example, 10.4 Mg $ha^{-1}yr^{-1}$ (Martinez et al., 2006), 21.5 Mg $ha^{-1}yr^{-1}$ (Gómez & Giráldez, 2007), 41.4 Mg $ha^{-1}yr^{-1}$ (Bruggeman et al., 2005) or 50 Mg $ha^{-1}yr^{-1}$ (Karamesouti et al., 2015). Such erosion rates should be reduced to a tolerable limit of around 1 Mg ha^{-1} yr^{-1} (Verheijen et al., 2009), especially for degraded shallow soils.

One of the effects of soil loss is the low C Stock; on average, 38 Mg ha^{-1} of C stock was observed in the 30 cm of soil depth in this study. It concurs with the range of C Stock from the study of 45 different soil profiles in the olive groves in Spain that is 39.9 ± 28.3 Mg ha^{-1} over 1 m depth (Rodríguez-Murillo, 2001). This range is considered low according to the global estimates

Table 4
Factor coordinates of the variables, correlations with three main factors and variance explained. On the left the principal component analysis (PCA) performed with samples between 0 to 10 and 10–20 cm depth; on the right, the PCA performed only with samples taken at 20–30 cm depth. Physical-Chemical soil variables were carbon stock in Mg ha-1 (C-Stock); Available water capacity (AWC), Gypsum (Sqtr.Gyps). The slope and tree's Diameters were also considered. The Indices calculated in the Sentinel-2 image (date 2017-11-15) with SNAP software were Brightness Index (BI_S-2), Shape Index (FI_S-2); Normalized Difference Vegetation Index (NDVI_S-2), and finally, the same indices were calculated from the blue, green, red and infra-red wavelengths obtained with the analytical spectral device, BI_ASD; FI_ASD and NDVI_ASD.

Variables	*0 to* 20 cm *depth* *Frequently tilled*			*20 to* 30 cm *depth* *Untilled*		
	Factor 1	Factor 2	Factor 3	Factor 1	Factor 2	Factor 3
Slope%	0,58	0,72	−0,28	0,44	0,83	0,18
Tree Diameter	−0,70	0,43	0,54	−0,76	0,05	0,60
C Stock Mg/ha	−0,86	0,21	−0,07	−0,88	0,32	0,04
AWC m^3/m^3	−0,79	0,23	−0,38	−0,71	0,40	−0,53
Sqr Gyps	0,77	0,32	0,23	0,82	0,29	0,04
BI_S-2	0,14	−0,26	−0,16	0,20	−0,20	−0,18
FI_S-2	−0,27	0,46	0,03	−0,22	0,27	0,30
NDVI_S-2	−0.38	0.22	0.18	−0.38	0.08	0.22
BI_ASD	0,48	−0,05	0,13	0,25	−0,20	−0,06
FI_ASD	−0,68	0,16	0,01	−0,75	0,11	0,08
NDVI_ASD	−0.72	0.34	−0.08	−0.66	0.15	0.32
% Total variance	55.3	18.0	11.6	54.5	20.9	13.7
Cumulative %	55.3	73.3	84.9	54.5	75.4	89.1

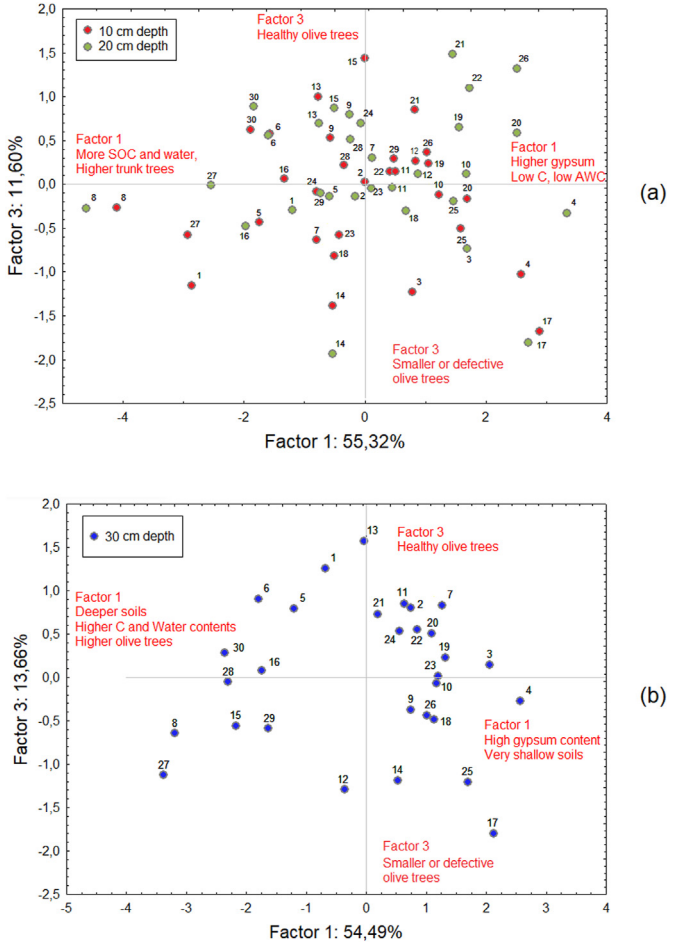

Fig. 5. Projection of soil samples on the plane formed by PCA Factors. Samples taken at 0–10 and 10–20 cm depth are represented at the upper figure (a). Samples taken at 10–30 cm depth are represented at the bottom figure (b).

elaborated by the FAO (2017). For a 30 cm depth, the C stock ranges from 20 to 120 Mg ha^{-1}. Concurrently, the available water content (AWC) declines. Olive trees are not water-demanding plants, and they can grow in different types of soils, producing fruits in areas with less than 200 mm of annual rainfall (Gucci & Fereres, 2012), although the optimal condition is around 600 mm of annual precipitation. However, water shortages and soil quality impact the plant vigor and survival rate (Sibbett & Osgood, 2004). Olive production in these soils, considering the average of good and bad years, is between 12 and 15 kg per tree (data not published). Production depends on the climate, soil, age, and tree variety. However, these figures are comparable with the olive production of different varieties growing in other drylands with less than 250 mm of annual rainfall with a maximum production of around 10.6 kg per tree (Aïachi Mezghani et al., 2019). The production is, however, lower than the yields of olive trees in highly productive irrigated areas and better soils that reach an average of 50 kg per tree (FAO, n.d.).

Several issues are damaging the development and production of olive trees, and all are interrelated: for example, low SOC hampers soil structure and decreases soil's ability to hold water (Castro et al., 2008; Palese et al., 2014); a high gypsum content results in an increase of water volume unavailable to the plants at the Permanent Wilting Point. Reported publications also describe the negative impact of gypsum on water availability (Moret-Fernandez & Herrero, 2015). The shallow soils, technically not very suitable for growing crops, become marginal when the first centimeters of soils are lost. In addition, when gypsum content exceeds 35%, water availability drops under 10% (Boyadgiev, 1974). Similar results were noticed in the soils of this study; soil layers under 20 cm depth showed AWC of 10%. Furthermore, over this depth, the massive Cy horizons were preventing further water availability and root development, which are usually extended only on the upper layers of soils (Parra-Rincón et al., 2002). The complex topography of the plot in this study created three micro-watersheds experiencing sediment loss and sediment deposition at different sites, leading to an accumulation of soil organic carbon (SOC), fine particles (silt and clay), and water in certain areas. In these sediment sinks, we could find better soil conditions (Hill & Schütt, 2000) and, therefore, favorable conditions for olive tree development. These areas showed lower reflectance compared to the upslope areas.

The described processes and changes can be monitored using remote sensing indices (Dorigo et al., 2007). The correlations between the indices derived from the S-2 image spectral data and the ASD laboratory-measured spectral data were significant (between

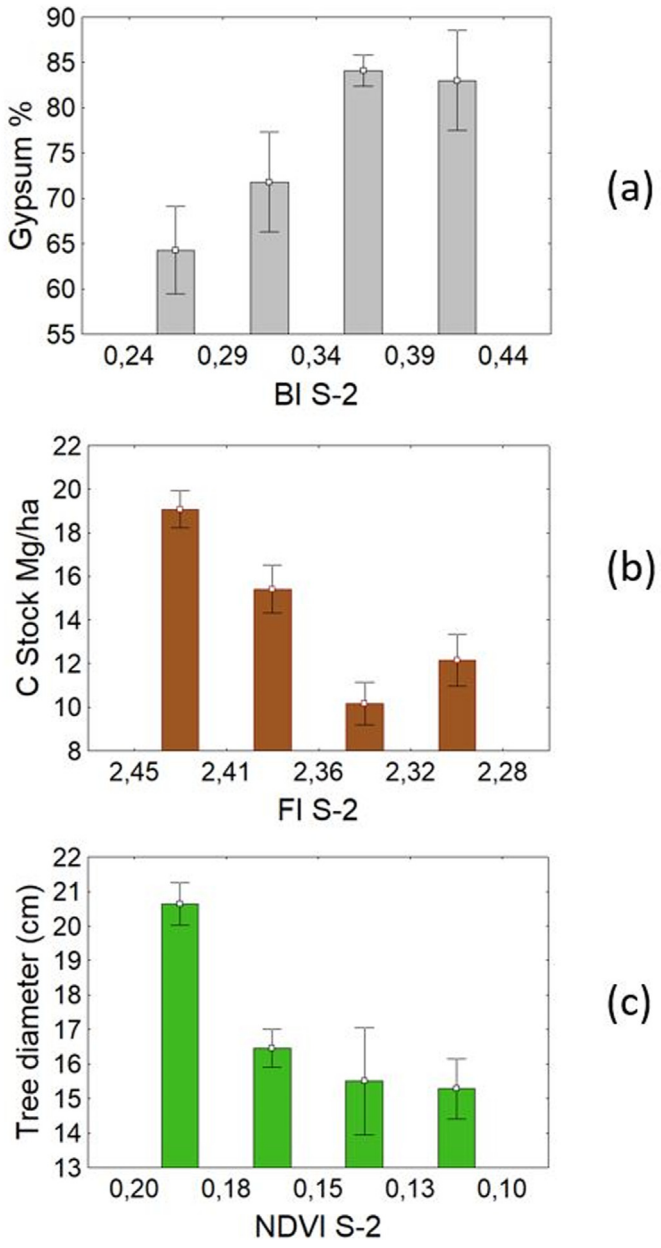

Fig. 6. From left to right the effect of soil erosion on the variables. Mean and standard error of Gypsum content (a), Carbon Stock (b) and Tree diameter (c) and the corresponding remote sensing indices derived by Sentinel 2 image: Brightness Index (BI), Shape Index (FI) and Normalized Difference Vegetation Index (NDVI).

0.39 and 0.49). Their contributions to the PCA was similar, as can be observed from Table 4. In sparse or low vegetative areas, like this olive grove, the influence of soil on reflectance values is very strong. From the PCA results, it was concluded that BI-ASD was more related to the gypsum content. Given the influence of the topography on the presence of gypsum at the topsoil, it was not surprising that the BI_S-2 was related to the slope of the plot.

The gypsiferous soils show a wide range of colors, moderately dark such as 10 YR 5/3 with less gypsum or light colors such as 2.5Y 8/1, which is due to the high gypsum content of Cy1 horizon. These colors are easily observed in the satellite imagery, especially when gypsum forms crusts, whose high reflectance is noticed if soils have more than 70% gypsum content (Escadafal et al., 1994, pp. 253–259). As a result, high gypsum content in the topsoil can be an indicator of soil degradation and desertification by erosion (Khanamani et al., 2017). In this study, the BI was related to the gypsum content, and the FI was related to the C stock, especially FI_ASD; studies have established the relationship between the shape of the spectral signatures and SOC (Henderson et al., 1992; Summers et al., 2011) which influences, in turn, the hue of soils.

The NDVI has been used as a proxy of net primary production; therefore, it is used to assess the health and coverage of vegetation (Higginbottom & Symeonakis, 2014). This index can be influenced by soil background reflectance in scarcely vegetated areas (Tucker et al., 1985); however, it has also been used to estimate soil texture and water content (Lozano-García et al., 1991), moisture in shallow soils (Wang et al., 2007), nitrogen and C content in soils (Sumfleth & Duttmann, 2008), and soil color, especially hue (Singh et al., 2006). From Fig. 3 it can be observed that the NDVI_S-2 is related to the tree diameter that indicates the plant vigor. However, these soils had a vegetation cover of around 20%, so the effect of soil reflectance was also prominent. However, the NDVI_ASD, calculated from soil samples measured at the laboratory, could not represent the plant vigor, and this index was more related to the SOC and AWC (Fig. 3). In general, the results of PCA were similar for the two depths of study (0–20 and 20–30 cm). Reflectance gathered by the S-2 images refer to the upper millimeters of soil; however, the results obtained in this study showed that soil characteristics over the 30 cm depth had a general influence on the soil surface and could be indicated by the vigor of trees, which was greater in areas with lower reflectance. These areas received sediment deposition from upper sites and had more SOC and AWC.

Tillage practices mix soil horizons; therefore, the gypsum accumulated in the C horizon was progressively more abundant in the upper layers, especially in the most eroded areas of the plot. Fig. 5 (a) shows the more homogeneous characteristics of soil samples in the upper layers (0–20 cm); these samples were, therefore, homogeneously distributed in the plane formed by the PCA Factors. On the contrary, the analysis performed with samples of the deepest layer (20–30 cm), as shown in Fig. 5 (b), resulted in a heterogeneous distribution of samples in the plane of Factors, i.e., none of the samples were located at the origin of the axes. This fact indicated that in the deeper layers (untilled), soil characteristics were more different between samples. In general, the PCA analysis separates different types of samples influenced by their position at the slope of the plot. Some samples showed lighter colors at the upper layers, but are darker in the layer underneath. This might be because they were located in areas receiving eroded sediments from higher topographic positions with lighter colors. However, high SOC and AWC in the deeper layers facilitated large trunk diameters, for example; this was the case with samples 12 and 21. Other areas showed soils with high reflectance in all the three layers considered. They are shown at the lower right quadrant of Fig. 5. The areas had trees with smaller trunk diameter as they were growing on layers close to the massive Cy horizon with water limitations. This Figure shows that soil changes according to the position on the connectivity system of this plot modeled by erosion processes depending on the topographic position and the degree of slope (Marques et al., 2020). In the present study, there was considerable variation between samples in the same plot; however, three thematic indices could establish the different influences of water erosion globally evidenced in tree development. The degraded soils evidenced less growing of olive trees that could be detected by an NDVI value of less than 0.18. The impact of soil degradation on the size of trees was also visible in the aerial photographs (Fig. 3).

The analysis of temporal variations of the thematic indices derived from temporal remote sensing images can be used for monitoring degradation or recovery of this type of soil if changes

are made in the land management practices. Agronomic productivity is related to water availability and SOC (Reeves, 1997); however, there are not many studies to relate agronomic productivity and erosion (Pimentel et al., 1995). The consequences have been revealed in this study; this aspect of erosion can be more effective to get the involvement of farmers who, according to surveys in the region, think that tillage prevents erosion (Marques et al., 2015) and are more worried about water and production then they are about soil erosion (Barbero-Sierra et al., 2018).

5. Conclusion

In the shallow soils of the study area with markedly differing horizons, tillage practices exposed different colors or hues at the surface that are indicative of the erosive processes. Certain hues at the surface indicate soil horizons that are not suitable for plant growth and can be observed by remote sensing. According to the PCA results, in these gypsiferous soils, the Brightness Index was related to the gypsum content, the increasing concentration of which decreases the amount of available water in the soil. The relationship between water content and soil organic carbon was also verified. The latter could be observed with the Shape Index. The NDVI, normally used as a vegetation index, was an indicator of soil and crop degradation in these sparsely vegetated soils of the study area. These three indices are recommended for monitoring changes and can be related to loss of water availability and crop productivity. The information can be used to increase awareness among land users, instead of figures of tons per hectare of soil loss.

Acknowledgements

This research was funded by the Project ACCION, and is part of the Operative Group Leñosot, supported by the Rural Development Programme 2014–2020 of the Comunidad de Madrid Government (Spain). We thank the cooperation of the Finca La Chimenea staff and the work of undergraduate students from the Autonomous University of Madrid.

References

Aïachi Mezghani, M., Mguidiche, A., Allouche Khebour, F., Zouari, I., Attia, F., & Provenzano, G. (2019). Water status and yield response to deficit irrigation and fertilization of three olive oil cultivars under the semi-arid conditions of Tunisia. *Sustainability, 11*(17). https://doi.org/10.3390/su11174812

Barbero-Sierra, C., Perez, M. R., Perez, M. J. M., Gonzalez, A. M. A., & Macein, J. L. C. (2018). Local and scientific knowledge to assess plot quality in Central Spain. *Arid Land Research and Management, 32*(1), 111–129. https://doi.org/10.1080/15324982.2017.1377781

Beaulieu, A., & Gaonac'h, H. (2002). Scaling of differentially eroded surfaces in the drainage network of the Ethiopian Plateau. *Remote Sensing of Environment, 82*(1), 111–122. https://doi.org/10.1016/S0034-4257(02)00028-7

Ben-Dor, E., Levin, N., Singer, A., Karnieli, A., Braun, O., & Kidron, G. J. (2006). Quantitative mapping of the soil rubification process on sand dunes using an airborne hyperspectral sensor. *Geoderma, 131*(1–2), 1–21. https://doi.org/10.1016/j.geoderma.2005.02.011

Bennett, S. J., & Wells, R. R. (2019). Gully erosion processes, disciplinary fragmentation, and technological innovation. *Earth Surface Processes and Landforms, 44*(1), 46–53. https://doi.org/10.1002/esp.4522

Bienes, R., & Marques, M. J. (2008). *Rill and interrill erosion produced by a single-storm event in an olive grove in central Spain*. EUROSOIL.

Bocco, G., & Valenzuela, C. R. (1993). Integrating satellite-remote sensing and geographic information systems technologies in gully erosion research. *Remote Sensing Reviews, 7*(3–4), 233–240. https://doi.org/10.1080/02757259309532179

Borrelli, P., Robinson, D. A., Fleischer, L. R., Lugato, E., Ballabio, C., Alewell, C., Meusburger, K., Modugno, S., Schuett, B., Ferro, V., Bagarello, V., Van Oost, K., Montanarella, L., & Panagos, P. (2017). An assessment of the global impact of 21st century land use change on soil erosion. *Nature Communications, 8*. https://doi.org/10.1038/s41467-017-02142-7

Boyadgiev, T. G. (1974). *Contribution to the knowledge of gypsiferous soils*. AGON/SF/SYR/67/522. Rome: FAO.

Bruggeman, A., Masri, Z., Turkelboom, F., Zöbisch, M., & El-Naheb, H. (2005). Strategies to sustain productivity of olive groves on steep slopes in the northwest of the Syrian Arab Republic. In J. Benites, M. Pisante, & F. Stagnari (Eds.), *Integrated soil and water management for orchard development: Role and importance* (Vol. 10, pp. 75–87). FAO. Land and Water Bulletin.

Castaldi, F., Palombo, A., Santini, F., Pascucci, S., Pignatti, S., & Casa, R. (2016). Evaluation of the potential of the current and forthcoming multispectral and hyperspectral imagers to estimate soil texture and organic carbon. *Remote Sensing of Environment, 179*, 54–65. https://doi.org/10.1016/j.rse.2016.03.025

Castro, J., Fernández-Ondoño, E., Rodríguez, C., Lallena, A. M., Sierra, M., & Aguilar, J. (2008). Effects of different olive-grove management systems on the organic carbon and nitrogen content of the soil in Jaén (Spain). *Soil and Tillage Research, 98*(1), 56–67. https://doi.org/10.1016/j.still.2007.10.002

Condit, H. R. (1970). The spectral reflectance of American Soils. *Photogrammetric Engineering, 36*(9), 955–966.

Dematte, J. A. M., Campos, R. C., Alves, M. C., Fiorio, P. R., & Nanni, M. R. (2004). Visible-NIR reflectance: A new approach on soil evaluation. *Geoderma, 121*(1–2), 95–112. https://doi.org/10.1016/j.geoderma.2003.09.012

Dorigo, W. A., Zurita-Milla, R., de Wit, A. J. W., Brazile, J., Singh, R., & Schaepman, M. E. (2007). A review on reflective remote sensing and data assimilation techniques for enhanced agroecosystem modeling. *International Journal of Applied Earth Observation and Geoinformation, 9*(2), 165–193. https://doi.org/10.1016/j.jag.2006.05.003

Dubovyk, O. (2017). The role of remote sensing in land degradation assessments: Opportunities and challenges. *European Journal of Remote Sensing, 50*(1), 601–613. https://doi.org/10.1080/22797254.2017.1378926

Dwivedi, R. S., & Ramana, K. V. (2003). The delineation of reclamative groups of ravines in the Indo-Gangetic alluvial plains using IRS-ID LISS-III data. *International Journal of Remote Sensing, 24*(22), 4347–4355. https://doi.org/10.1080/0143116031000116994

D'Odorico, P., Bhattachan, A., Davis, K. F., Ravi, S., & Runyan, C. W. (2013). Global desertification: Drivers and feedbacks. *Advances in Water Resources, 51*, 326–344. https://doi.org/10.1016/j.advwatres.2012.01.013

ESA. (2015). Sentinel-2 user handbook. In *ESA standard document* (p. 64). European Space Agency. https://sentinel.esa.int/documents/247904/685211/Sentinel-2_User_Handbook.

Escadafal, R. (1989). Remote sensing of arid soil surface color with Landsat thematic mapper. *Advances in Space Research, 9*(1), 159–163. https://doi.org/10.1016/0273-1177(89)90481-X

Escadafal, R., Belghith, A., & Ben Moussa, H. (1994). *Indices spectraux pour la dégradation des milieux naturels en Tunisie aride. 6ème Symp. Int. Mesures Physiques et Signatures En Télédétection*. ISPRS-CNES.

FAO. (2017). *Global soil organic database (at 30 arcsec)*. FAO and Euro-Mediterranean Center on Climate Change Foundation. http://www.fao.org/3/a-i7292e.pdf.

FAO. (n.d.). *Data bases & software. Olive. Yield*. Land & water. Retrieved February 3, 2020, from http://www.fao.org/land-water/databases-and-software/crop-information/olive/en/.

Fleskens, L., & Stroosnijder, L. (2007). Is soil erosion in olive groves as bad as often claimed? *Geoderma, 141*(3–4), 260–271. https://doi.org/10.1016/j.geoderma.2007.06.009

Franklin, J. A. (1977). Suggested methods for determining water content, porosity, density, absorption and related properties (Part 1). In I. Pergamon Press (Ed.), *Suggested methods for determining water content, porosity density, absorption and related properties and swelling and slake-durability index properties* (pp. 141–151). International Society for Rock Mechanics. Commission on Standardization of Laboratory and Field Tests.

Franzini, M., & Lezzerini, M. (2003). A mercury-displacement method for stone bulk-density determinations. *European Journal of Mineralogy, 15*, 225–229. https://doi.org/10.1127/0935-1221/2003/0015-0225

Galvão, L. S., Formaggio, A. R., Couto, E. G., & Roberts, D. A. (2008). Relationships between the mineralogical and chemical composition of tropical soils and topography from hyperspectral remote sensing data. *ISPRS Journal of Photogrammetry and Remote Sensing, 63*(2), 259–271. https://doi.org/10.1016/j.isprsjprs.2007.09.006

Gómez, J. A., Battany, M., Renschler, C. S., & Fereres, E. (2003). Evaluating the impact of soil management on soil loss in olive orchards. *Soil Use & Management, 19*(2), 127–134. https://doi.org/10.1111/j.1475-2743.2003.tb00292.x

Gómez, J. A., & Giráldez, J. V. (2007). *Soil and water conservation. A European approach through ProTerra projects* (Proceedings of the European Congress on Agriculture and the Environment).

Gomez, C., Viscarra Rossel, R. A., & McBratney, A. B. (2008). Soil organic carbon prediction by hyperspectral remote sensing and field vis-NIR spectroscopy: An Australian case study. *Geoderma, 146*(3–4), 403–411. https://doi.org/10.1016/J.GEODERMA.2008.06.011

de Graaff, J., Duran Zuazo, V.-H., Jones, N., & Fleskens, L. (2008). Olive production systems on sloping land: Prospects and scenarios. *Journal of Environmental Management, 89*(2, SI), 129–139. https://doi.org/10.1016/j.jenvman.2007.04.024

Gucci, R., & Fereres, D. (2012). Olive. In P. Steduto, T. C. Hsiao, D. Fereres, & D. Raes (Eds.), *Crop yield response to water. FAO irrigation and drenage paper. No. 66* (pp. 300–313). FAO.

Henderson, T. L., Baumgardner, M. F., Franzmeier, D. P., Stott, D. E., & Coster, D. C. (1992). High dimensional reflectance analysis of soil organic matter. *Soil Science Society of America Journal, 56*, 865–872. https://doi.org/10.2136/sssaj1992.03615995005600030031x

Hernandez, A. J., Lacasta, C., & Pastor, J. (2005). Effects of different management practices on soil conservation and soil water in a rainfed olive orchard. *Agricultural Water Management, 77*(1–3), 232–248. https://doi.org/10.1016/

j.agwat.2004.09.030
Higginbottom, T. P., & Symeonakis, E. (2014). Assessing land degradation and desertification using vegetation index data: Current frameworks and future directions. *Remote Sensing, 6*(10), 9552–9575. https://doi.org/10.3390/rs6109552
Hill, J., Megier, J., & Mehl, W. (1995). Land degradation, soil erosion and desertification monitoring in Mediterranean ecosystems. *Remote Sensing Reviews, 12*(1–2), 107–130. https://doi.org/10.1080/02757259509532278
Hill, J., & Schütt, B. (2000). Mapping complex patterns of erosion and stability in dry mediterranean ecosystems. *Remote Sensing of Environment, 74*(3), 557–569. https://doi.org/10.1016/S0034-4257(00)00146-2
Huete, A., Justice, C., & Liu, H. (1994). Development of vegetation and soil indices for MODIS-EOS. *Remote Sensing of Environment, 49*(3), 224–234. https://doi.org/10.1016/0034-4257(94)90018-3
Instituto Geográfico Nacional. (2014). Instituto Geográfico nacional. Plan nacional de Ortofotografía aérea PNOA. In *Ministerio de Fomento de España*. http://centrodedescargas.cnig.es/CentroDescargas/index.jsp.
IPCC. (2006). *Intergovernmental Panel on climage change guidelines for national greenhouse gas inventories*. National Greenhouse Gas Inventories Programme. Institute for Global Environmental Strategies (IGES) https://www.ipcc-nggip.iges.or.jp/public/2006gl/.
Karamesouti, M., Detsis, V., Kounalaki, A., Vasiliou, P., Salvati, L., & Kosmas, C. (2015). Land-use and land degradation processes affecting soil resources: Evidence from a traditional Mediterranean cropland (Greece). *Catena, 132*, 45–55. https://doi.org/10.1016/j.catena.2015.04.010
Khanamani, A., Fathizad, H., Karimi, H., & Shojaei, S. (2017). Assessing desertification by using soil indices. *Arabian Journal of Geosciences, 10*(13). https://doi.org/10.1007/s12517-017-3054-5
Klug, H. P., & Alexander, L. E. (1974). *X-ray diffraction procedures for polycrystalline and amorphous materials* (2nd ed.). Wiley.
Lee, H., & Liu, J. G. (2001). Analysis of topographic decorrelation in SAR interferometry using ratio coherence imagery. *IEEE Transactions on Geoscience and Remote Sensing, 39*(2), 223–232. https://doi.org/10.1109/36.905230
Lozano-García, D. F., Fernández, R. N., & Johannsen, C. J. (1991). Assessment of regional biomass-soil relationships using vegetation indexes. *IEEE Transactions on Geoscience and Remote Sensing, 29*(2), 331–339. https://doi.org/10.1109/36.73676
Marques, M. J., Álvarez, A. M., Carral, P., Esparza, I., Sastre, B., & Bienes, R. (2020). Estimating soil organic carbon in agricultural gypsiferous soils by diffuse reflectance spectroscopy. *Water, 12*(1), 261. https://doi.org/10.3390/w12010261
Marques, M. J., Bienes, R., Cuadrado, J., Ruiz-Colmenero, M., Barbero-Sierra, C., & Velasco, A. (2015). Analysing perceptions attitudes and responses of wine-growers about sustainable land management in Central Spain. *Land Degradation & Development, 26*(5). https://doi.org/10.1002/ldr.2355
Martinez, J. R. F., Zuazo, V. H. D., & Raya, A. M. (2006). Environmental impact from mountainous olive orchards under different soil-management systems (SE Spain). *The Science of the Total Environment, 358*(1–3), 46–60. https://doi.org/10.1016/j.scitotenv.2005.05.036
McCarty, G. W., Reeves, J. B., Reeves, V. B., Follett, R. F., & Kimble, J. M. (2002). Mid-infrared and near-infrared diffuse reflectance spectroscopy for soil carbon measurement. *Soil Science Society of America Journal, 66*(2), 640–646. https://doi.org/10.2136/sssaj2002.0640
Metternicht, G. I., & Zinck, J. A. (2003). Remote sensing of soil salinity: Potentials and constraints. *Remote Sensing of Environment, 85*(1), 1–20. https://doi.org/10.1016/s0034-4257(02)00188-8
Moret-Fernandez, D., & Herrero, J. (2015). Effect of gypsum content on soil water retention. *Journal of Hydrology, 528*, 122–126. https://doi.org/10.1016/j.jhydrol.2015.06.030
Palese, A. M., Vignozzi, N., Celano, G., Agnelli, A. E., Pagliai, M., & Xiloyannis, C. (2014). Influence of soil management on soil physical characteristics and water storage in a mature rainfed olive orchard. *Soil and Tillage Research, 144*, 96–109. https://doi.org/10.1016/j.still.2014.07.010
Panagos, P., Borrelli, P., Meusburger, K., Alewell, C., Lugato, E., & Montanarella, L. (2015). Estimating the soil erosion cover-management factor at the European scale. *Land Use Policy, 48*, 38–50. https://doi.org/10.1016/j.landusepol.2015.05.021
Parra Rincón, M. A., Fernández-Escobar, R., Navarro García, C., & Arquero, O. (2002). *Los suelos y la fertilización del olivar cultivado en zonas calcáreas*. Mundi Prensa.
Pimentel, D., Harvey, C., Resosudarmo, P., Sinclair, K., Kurz, D., Mcnair, M., Crist, S., Shpritz, L., Fitton, L., Saffouri, R., & Blair, R. (1995). Environmental and economic costs OF soil erosion and conservation benefits. *Science, 267*(5201), 1117–1123. https://doi.org/10.1126/science.267.5201.1117
QGIS. (n.d.). Geographic information system. OpenSource geospatial foundation Project. v2.3.0.Chugiak.
Reeves, D. W. (1997). The role of soil organic matter in maintaining soil quality in continuous cropping systems. *Soil and Tillage Research, 43*(1–2), 131–167. https://doi.org/10.1016/S0167-1987(97)00038-X
Richards, L. A. (1941). A pressure-membrane extraction apparatus for soil solution. *Soil Science, 51*(1), 377–386. https://doi.org/10.1097/00010694-194105000-00005
Rodríguez-Murillo, J. C. (2001). Organic carbon content under different types of land use and soil in peninsular Spain. *Biology and Fertility of Soils, 33*(1), 53–61. https://doi.org/10.1007/s003740000289
Rojas, R. V., Achouri, M., Maroulis, J., & Caon, L. (2016). Healthy soils: A prerequisite for sustainable food security. *ENVIRONMENTAL EARTH SCIENCES, 75*(3). https://doi.org/10.1007/s12665-015-5099-7
Sabins, F. F. (1999). Remote sensing for mineral exploration. *Ore Geology Reviews, 14*(3–4), 157–183. https://doi.org/10.1016/S0169-1368(99)00007-4
Sastre, B. (2017). Estimating soil redistribution rates in an agricultural hillside by 137Cs: Case study in Central Spain on gypsiferous soil. In U. de Alcalá (Ed.), *Empleo de Cubiertas vegetales en olivar, repercusión sobre el suelo, la erosión y la calidad del aceite de oliva virgen* (pp. 40–61). Universidad de Alcalá.
Sastre, B., Barbero-Sierra, C., Bienes, R., Marques, M. J., & García-Díaz, A. (2017). Soil loss in an olive grove in Central Spain under cover crops and tillage treatments, and farmer perceptions. *Journal of Soils and Sediments, 17*(3). https://doi.org/10.1007/s11368-016-1589-9
Schulte, E. E., & Hopkins, B. G. (1996). Estimation of organic matter by weight loss-on-ignition. In F. R. Magdoff, M. A. Tabatabai, & E. A. Hanlon, Jr. (Eds.), *Soil organic matter: Analysis and interpretation* (pp. 21–31). SSSA Special Publication.
Shepherd, K. D., & Walsh, M. G. (2002). Development of reflectance spectral libraries for characterization of soil properties. *Soil Science Society of America Journal, 66*(3), 988–998.
Sibbett, G. S., & Osgood, J. (2004). *Olive production manual*. In G. S. Sibbett, & L. Ferguson (Eds.) (2nd., pp. 27–34). Oakland, Calif: University of California. Agriculture and Natural Resources.
Singh, D., Meirelles, M. S. P., Costa, G. A., Herlin, I., Berroir, J. P., & Silva, E. F. (2006). Environmental degradation analysis using NOAA/AVHRR data. *Advances in Space Research, 37*(4), 720–727. https://doi.org/10.1016/j.asr.2004.12.052
SNAP-ESA. Sentinel application Platform v7.0.2. http://setp.esa.int.
SPSS-Inc. (2009). *PASW statistics for windows*. SPSS Inc.
Sumfleth, K., & Duttmann, R. (2008). Prediction of soil property distribution in paddy soil landscapes using terrain data and satellite information as indicators. *Ecological Indicators, 8*(5), 485–501. https://doi.org/10.1016/j.ecolind.2007.05.005
Summers, D., Lewis, M., Ostendorf, B., & Chittleborough, D. (2011). Visible near-infrared reflectance spectroscopy as a predictive indicator of soil properties. *Ecological Indicators, 11*(1), 123–131. https://doi.org/10.1016/j.ecolind.2009.05.001
Symeonakis, E., & Drake, N. (2004). Monitoring desertification and land degradation over sub-Saharan Africa. *International Journal of Remote Sensing, 25*(3), 573–592. https://doi.org/10.1080/0143116031000095998
Tivet, F., Sá, J. C., de, M., Lal, R., Briedis, C., Borszowskei, P. R., dos Santos, J. B., Farias, A., Eurich, G., da Cruz Hartman, D., Junior, M. Nadolny, Bouzinac, S., & Séguy, L. (2013). Aggregate C depletion by plowing and its restoration by diverse biomass-C inputs under no-till in sub-tropical and tropical regions of Brazil. *Soil and Tillage Research, 126*, 203–218. https://doi.org/10.1016/j.still.2012.09.004
Tucker, C. J., Vanpraet, C. L., Sharman, M. J., & Van Ittersum, G. (1985). Satellite remote sensing of total herbaceous biomass production in the senegalese sahel: 1980-1984. *Remote Sensing of Environment, 17*(3), 233–249. https://doi.org/10.1016/0034-4257(85)90097-5
Verheijen, F. G. A., Jones, R. J. A., Rickson, R. J., & Smith, C. J. (2009). Tolerable versus actual soil erosion rates in Europe. *Earth-Science Reviews, 94*(1–4), 23–38. https://doi.org/10.1016/j.earscirev.2009.02.003
Vrieling, A. (2006). Satellite remote sensing for water erosion assessment: A review. *Catena, 65*(1), 2–18. https://doi.org/10.1016/J.CATENA.2005.10.005
Wang, X., Xie, H., Guan, H., & Zhou, X. (2007). Different responses of MODIS-derived NDVI to root-zone soil moisture in semi-arid and humid regions. *Journal of Hydrology, 340*(1–2), 12–24. https://doi.org/10.1016/j.jhydrol.2007.03.022
Whiting, M. L., Li, L., & Ustin, S. L. (2004). Predicting water content using Gaussian model on soil spectra. *Remote Sensing of Environment, 89*(4), 535–552. https://doi.org/10.1016/j.rse.2003.11.009
Wrb, I. (2015). *Reference Base for Soil Resources 2014, update 2015. International soil classification system for naming soils and creating legends for soil maps. No. 106.* FAO.